JOURNAL OF MATERIALS SCIENCE 11 (1976) 703–710

A method for the identification of crack-front location during fatigue fracture in polymers

V. I. SINGIAN, J. W. TEH, J. R. WHITE*
Department of Materials, Queen Mary College, London, UK

An attempt has been made to accurately locate the crack-front position at intervals during fatigue cycling of low density polyethylene specimens by means of markers. Scanning electron microscopy has been used to inspect the fracture surfaces and the markers have been identified by means of the X-ray image produced by the signal from a fully focusing crystal spectrometer.

1. Introduction

In most fracture mechanics analyses of slow or cyclic crack propagation the crack length itself is an important parameter. The crack length measurement is usually made at the specimen surface, to which there can be little objection when the specimen is thin; suitably chosen test-piece configurations can lead to particularly simple analyses. The implicit assumption that the crack front is straight can lead to a serious discrepancy between the true situation and the idealized model used for fracture mechanics when the specimen has finite thickness and the crack length is measured only at the surface. It may not be necessary to map out the development of the fracture front throughout propagation if the important parameters can be estimated by other means, for instance the area of the crack can be derived from conductivity measurements which can provide continual monitoring throughout the testing of a conducting specimen [1]. This technique is not available to non-conducting materials such as polymers.

The work described here was designed to complement studies by Andrews and others in this laboratory of fatigue fracture of semi-crystalline polymers [2, 3]. Walker noted that the crack front bowed strongly, with the centre leading [4]. Since his specimens were thin (usually 0.8 mm) the effect would probably not demand reassessment of the analysis of his results, except at small crack lengths. The test-piece configuration employed in the reversed loading studies [3] has a square cross-section (3 mm × 3 mm) on the other hand, and it has become clear on attempting to perform a fracture mechanics analysis on the data, that details of the crack front profile need to be known. This profile will, of course, partially reflect the stress distribution which itself will be complicated for non-linear viscoelastic specimens of the test-piece geometry used, and some of the simplifications allowed in fracture mechanics analyses of simpler arrangements are excluded. A discussion of this topic will be included in a later paper.

A method of marking the fracture front has been developed which involves interrupting the test and evaporating metal into the crack to deposit onto the fracture surfaces. Control experiments have been conducted using other marking techniques to investigate the validity of this procedure.

2. Experimental

2.1. Deformation cycling

Uniaxial tensile strain cycling tests were conducted on the machine described in detail previously [3]. Dumb-bell specimens of low density polyethylene with 10 mm gauge length of square cross-section (3 mm × 3 mm), were prepared as before [3]. An edge crack with its front parallel to the edge was initiated with a fresh razor blade prior to each test. At the strains used, 4 to 9%, crack propagation was rapid in the context of fatigue testing, and samples failed in less than 1000 cycles. The

* Present address: Department of Metallurgy and Engineering Materials, The University of Newcastle-upon-Tyne, UK.

cycling frequency of 0.25 Hz was chosen to preclude thermal effects.

2.2. Crack-front marking

2.2.1. Evaporated markers

Tests were interrupted at intervals, up to three times during a specimen lifetime, and the test-piece removed from the fatigue machine. The test-piece was immediately placed in a jig designed to hold it sufficiently under tension to hold the crack open and expose the fracture surfaces. The strain was chosen to be significantly less than the peak strain during fatigue cycling. The test-piece was then placed in an evaporation chamber, and metal evaporated into the crack. It was attempted to put an average coating of approximately 20 nm on the fracture surfaces, although control of the thickness is most inaccurate at the shallow angles of evaporation in this arrangement (Fig. 1). After evaporation, the test-piece was returned to the fatigue machine and deformation cycling continued as before. When more than one interruption/evaporation was performed, the heaviest element (gold) was used in the first evaporation and the lightest (aluminium) in the final one.

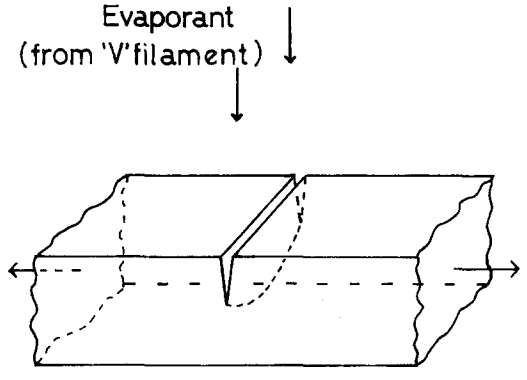

Figure 1 Evaporation arrangement. The evaporant is approximately 65 mm above the specimen surface.

2.2.2. Aerosol-propelled markers

While the evaporation technique provides the smallest available marker, and thus the best resolution, objections could be raised against the procedure used, involving interruption of deformation cycling and a prolonged static straining before recommencing. Dynamic marking was, therefore, attempted during the course of a limited number of control experiments. It was originally felt that aerosol-delivered sub-micron particles would be ideally suited to this application, but on making enquiries it soon became clear that the size distribution of aerosol particles is rarely known or available. Another problem is that most if not all aerosol propellants are potential stress corrosion agents for polyethylene. In the absence of a comprehensive survey of aerosol ingredients the choice was somewhat arbitrary, and a common anti-perspirant spray was employed. Control of the quantity of material deposited on the fracture surface was even more difficult here, but a short burst ($\sim \frac{1}{2}$ sec) directed into the crack from a distance of approximately 100 mm while the specimen was passing through the position of maximum strain was found to give the best results.

2.2.3. Air-borne particles

As an alternative to the aerosol technique for *in-situ* dynamic marking, free from the problem of stress corrosion, attempts were made to mark the crack front with small polishing particles, propelled into the crack by an air jet. Most experiments were conducted with jeweller's rouge.

2.3. Scanning electron microscopy

After completion of the test, both fracture surfaces were mounted on a brass stub and carbon-coated in preparation for viewing in a JEOL JXA-50A scanning electron microscope fitted with two fully focusing dual spectrometers for X-ray microanalysis. Carbon was chosen rather than one of the metals normally preferred for SEM observation of non-conducting surfaces to allow the location of the markers by their X-ray emission. In this technique the crystal spectrometer is set to detect a particular wavelength and each time an X-ray is counted a spot is plotted on the display screen at the position corresponding to the location of the scanning electron beam on the specimen. If the mass-thickness of the coating is too high the electron beam is so diminished on reaching the markers that the X-ray yield is insufficient to produce a tolerable exposure time. Too thin a film will result in serious specimen damage, although this may be informative if it develops slowly as in cases examined in Section 3.3. Some degree of compensation for an inappropriate coating thickness can be effected through the choice of the electron-beam accelerating potential, which can be varied continuously in the range 0 to 50 kV on the instrument employed here. The X-ray/spectrometer crystal combination for each element used is shown in Table I.

TABLE I X-ray imaging conditions

Element	Marker	X-ray line	Analysing crystal
Au	Evaporated metal	$L\alpha$	PET
Ag	Evaporated metal	$L\alpha$	PET
Al	Evaporated metal	$K\alpha$	RAP
Al	Aluminium chlorohydrate (aerosol particles)	$K\alpha$	RAP
Fe	Jeweller's rouge	$K\alpha_1$	PET

3. Results and discussion

3.1. General appearance of the crack front and fracture surface

The crack front was generally found to grow from the straight razor cut into a curved profile, with the centre growing faster intially. The surface measurement, therefore, represents the slowest actual rate of any part of the crack during the early stages of propagation. Fig. 2 is a secondary electron image (SEI) of part of a fracture surface onto which gold was evaporated after 434 deformation cycles, followed by silver (585) and aluminium (810). Sometimes the evaporated layer showed up clearly in the SEI, and could be seen also under a light microscope. An example is the gold layer in Fig. 2, which terminates at the front marked A . . . A. Details of the fracture surface beneath the gold layer have been partially obscured by it. Clearly a thinner layer, much closer to the threshold of visibility, would be preferred not only on the grounds of image quality in the region covered but also because a thinner layer would be less likely to modify the stress near the crack tip when it closes. Any such modification may alter the crack sharpening thought to occur during fatigue crack propagation, so modifying in turn the crack growth itself. Examples of thinner layers, probably near the optimal thickness are presented later.

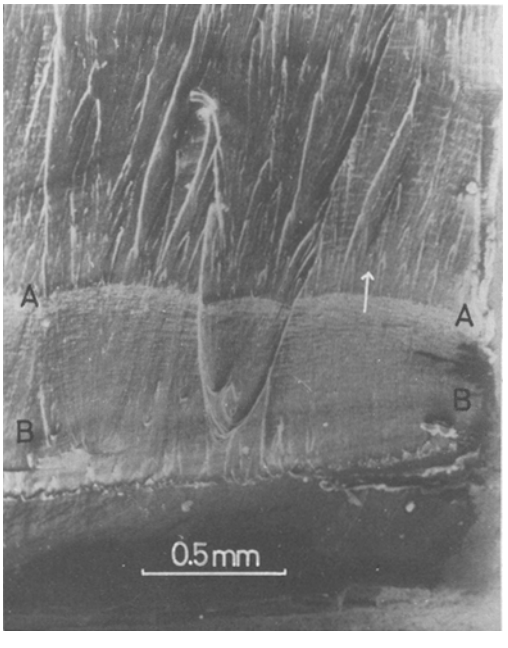

Figure 2 Fracture surface of LDPE with the position of the fracture front after 434 cycles of deformation marked with gold (A . . . A). The approximate position of the razor initiation is shown as B . . . B. The poor definition of the specimen boundaries, particularly in the bottom right-hand corner of the picture, results from deformation of the specimen during testing, and from the direction of viewing, with the electron beam normal to the specimen surface. The arrow indicates the direction of crack propagation.

Fatigue striations are visible on most of the fracture surfaces (Fig. 3). The number of striations has been found to correspond approximately to the total number of cycles to failure during the test whenever counted. On many fracture surfaces, striations which are much more prominent than their neighbours appear at intervals of between three and ten "primary" striations, as in Fig. 3. One possible explanation for this phenomenon is that the prominent striations correspond to actual crack front positions during the test, while the intermediate striations correspond to damage occurring in intervening deformation cycles with-

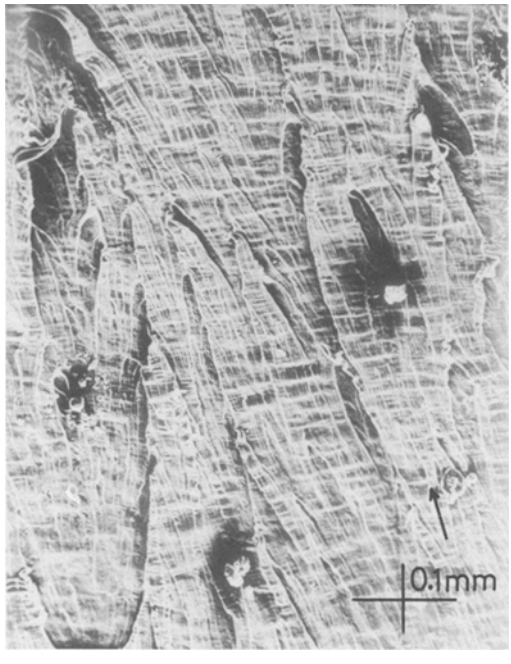

Figure 3 Fracture surface of LDPE coated with gold-palladium. Peak strain in tension 5.50%. Sample failed in 700 cycles.

out crack propagation. Other workers have observed polymer fatigue fracture surfaces with striation periods of the order of 100 times the average growth per cycle (see the comprehensive review by Manson and Hertzberg [5]). The explanation given is that the material ahead of the (temporarily stationary) crack becomes progressively weakened by the deformation cycling until the threshold condition for crack propagation is surmounted and it moves (in one cycle) to a new position at which it remains until the material now immediately ahead of it is sufficiently weakened to allow another jump. In this case the striations have been termed "arrest lines". Structure between arrest lines has not previously been reported to our knowledge.

Other fracture markings less numerous but more prominent than the fatigue striations are seen lying mainly in directions inclined $< 10^{\circ}$ to the crack propagation direction. They represent the boundaries between regions in which the crack grew at different levels, and sometimes occur in pairs, emerging from a common origin to form a parabolic apex directed anti-parallel to the crack propagation direction. There is often a discontinuity of the fracture front on crossing these markings; examples in which the front leads inside an associated pair of lines and others in which it lags behind inside the pair have been noted, (cf. Figs. 2 and 5a).

3.2. Detailed observations using evaporated metal markers

Although clear location of crack-front position was often achieved in the SEI, as in Fig. 2, the marking often remained undetected unless use was made of the X-ray image facility. In the case shown in Fig. 4 the evaporated aluminium layer thickness was probably near optimal. It is to be admitted that the majority of cases where this situation occurred were final (aluminium) markings. This is to be expected since the gold markers are beneath successive layers of silver, aluminium and carbon which, although lighter, will significantly reduce the signal-to-noise ratio even if the electron beam is still sufficiently energetic on reaching the gold to produce an X-ray signal at all. An example of near-optimal marking by gold and silver (also subsequently coated by aluminium and carbon), is shown in Fig. 5. The marking is visible in the SEI but does not seem to have obscured any detail, and indeed appears to be beneficial in Fig. 5c. A delicate balance between the thicknesses of the successive layers is evidently demanded.

The images confirm that the fatigue striations do indeed correspond to crack front positions.

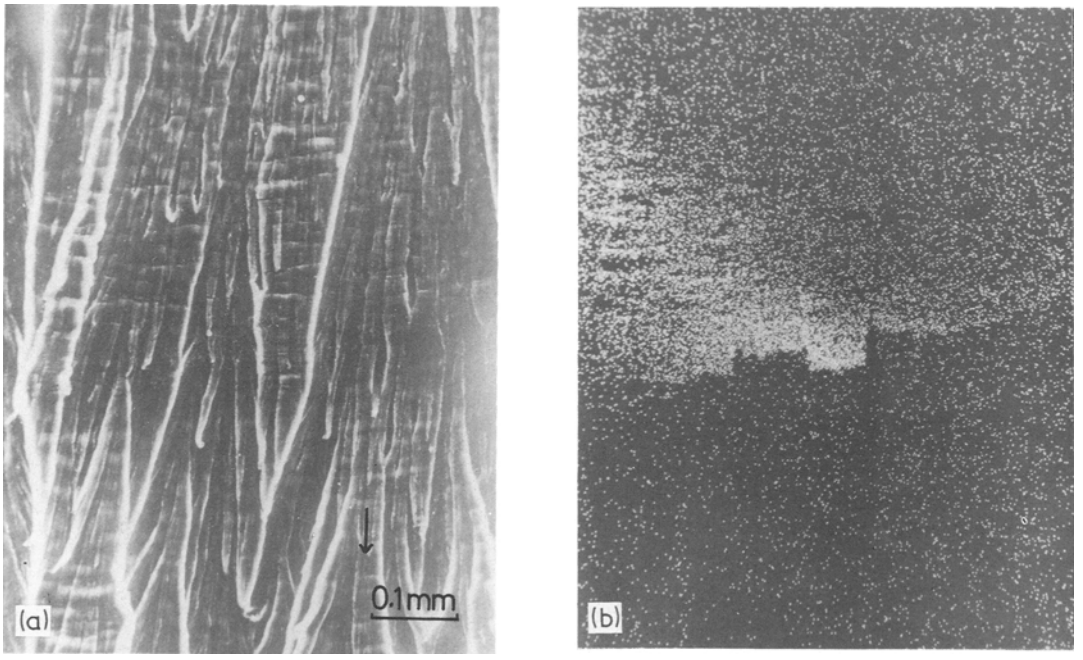

Figure 4 Another part of the fracture surface shown in Fig. 2. (a) SEI, (b) Al X-ray image. Aluminium evaporation was performed after 810 cycles.

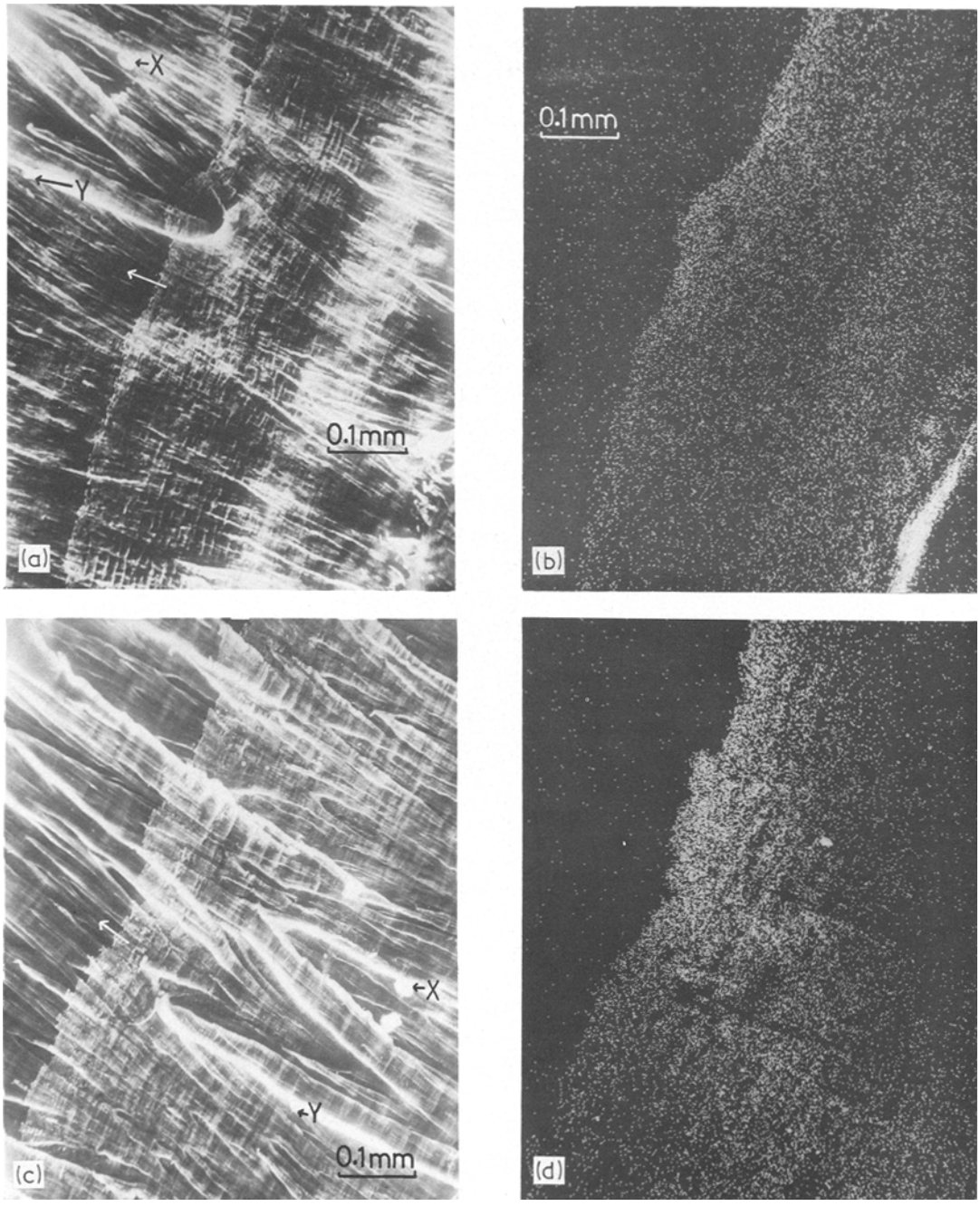

Figure 5 Parts of a fracture surface from a test at 4.75% strain marked with gold after 225 cycles, silver after 280 cycles, and aluminium after 350 cycles. (a) SEI showing the gold front, (b) Au X-ray image of the area shown in (a), (c) SEI of a neighbouring area containing the silver front, (d) Ag X-ray image of the area shown in (c). Note that the features at X and Y in (a) and (c) are common to both areas. (a) and (b) were recorded at 48 keV, (c) and (d) at 25 keV.

While it is hard to imagine otherwise it is interesting to observe the extent of departure of the crack front from linearity shown in Fig. 6, noting in particular that the route taken when crossing the gross markings which lie in the direction of crack propagation could hardly be deduced from the SEI. There is no break in the regularity, direction or period of the striation pattern across the marked boundary and there is no indication in the micrographs that any modification to crack propagation is caused by the interruption of deformation cycling nor by the presence of the evaporated

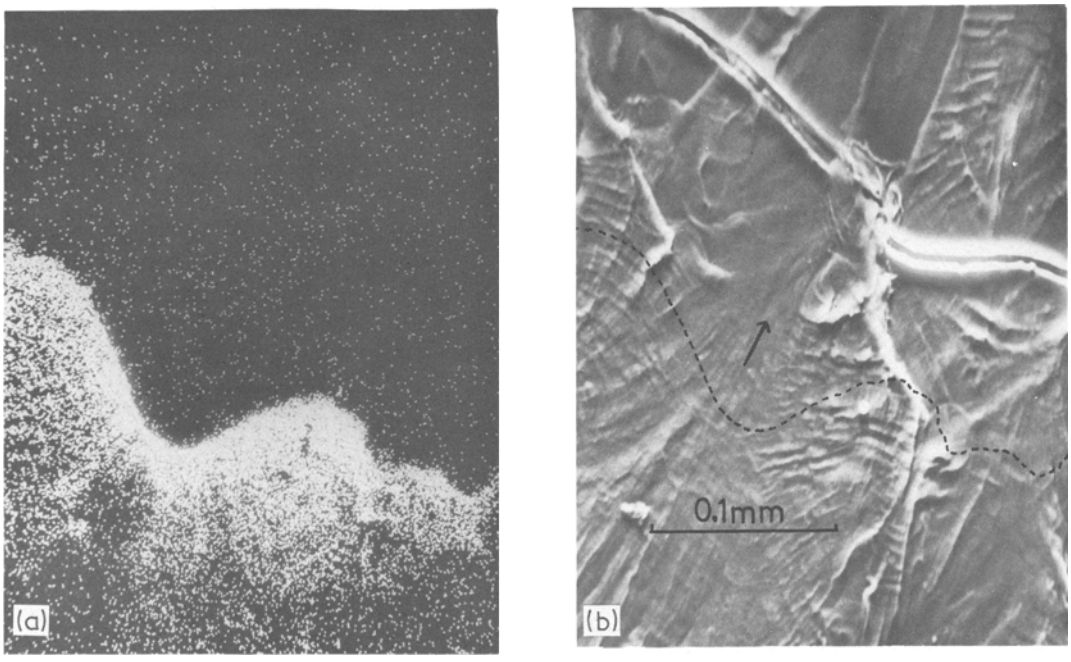

Figure 6 Part of an Al-marked fracture surface. (a) Al X-ray image, (b) SEI with traced position of fracture front at marking. The fissure which runs across the picture and is displaying charging is an artefact produced by irradiation, see Section 3.3.

metal layer.

Load–deformation characteristics recorded immediately before and after marking were usually not identical, although after a few cycles of post-marking deformation the characteristic returned to close similarity with the state just prior to the interruption. Creep of a magnitude close to that normally associated with the beginning of a test was found to occur after marking, indicating that sample relaxation had occurred during the interruption in cyclic testing. Creep would normally be very slow at the stage of the test at which marking is performed, and the variation in the load–deformation characteristics almost certainly derives from this source, rather than some direct interaction of the markers with the test-piece. (Description of the technique of creep detection and measurement is included in [3]). No evidence of modification to crack growth behaviour could be detected in plots of (surface) crack growth against number of cycles.

3.3. Growth of fissures in the electron beam

Polyethylene surfaces are normally prepared for SEM observation by coating with a continuous layer of a relatively heavy metal. This prevents charging and will also sufficiently diminish the electron beam before it reaches the polymer that melting will be minimized. The specimens described here rely ultimately on the final carbon coating for these purposes, yet this must be kept sufficiently thin to allow for X-ray image production. Metal layers are present over part of the specimen, but these are thin and may be distontinuous due to shadowing effects produced by the rough nature of the fracture combined with the unidirectional, shallow-angled evaporation arrangement used*. The coating layer thickness must, therefore, represent a compromise between the conflicting requirements of the X-ray image and minimization of radiation damage, and it has been found impossible to afford complete protection against damage while achieving adequate X-ray signals. In every case the damage took the form of shallow fissures, as already seen in Fig. 6. Severe charging usually surrounded the fissures leading to the belief that the coating film had probably broken to expose the polymer. The fissures grew only under prolonged exposure, as during the recording of an X-ray image, which usually required between 5 and 40 min at 2×10^{-8} A, and were

* This problem would probably be markedly reduced by sputtering rather than evaporating the marking layer. Control of thickness might be easier with this technique.

Figure 7 Another part of the specimen shown in Fig. 5. (a) SEI, (b) Ag X-ray image, (c) SEI of the same area after recording (b).

never nucleated while operating at the lower currents appropriate to secondary electron image observation. The development of a fissure during the recording of an X-ray image often produced a corresponding concentration of X-ray counts (Fig. 7) but was never found to confuse identification of the crack-front location.

More detailed studies of fissure formation in these and other specimens lead us to believe that they are promoted by the release of internal stresses, which accounts for their directional behaviour; they are always found to lie perpendicular to the direction of crack growth on the fatigue fracture surfaces.

3.4. The use of other marking techniques

The resolution of jeweller's rouge-marked crack-fronts is inferior to that obtained by evaporation. This may in part be caused by aggregation of the particles. There is nothing to indicate that this method offers any advantage, nor that the evaporation method introduces unwanted artefacts.

The results from aerosol marking experiments confirmed the difficulties attached to this technique. The propellant appeared to have caused swelling on some surfaces and such examples quickly deteriorated in the electron beam leading to serious charging as the conductive layer became disrupted, possibly due to the release of absorbed propellant. The load–deformation characteristic often showed a significant change on marking by this method, with the loads in both tension and compression taking higher values on the cycle immediately following the marking. The result recorded in tension probably derives from a weak solvent bonding action of the propellant, while the increase in compressive load can be explained by the extra strain which is produced by the included

marker particles. The experiments were often marred by the presence of unacceptably large marker particles ($\sim 5\,\mu m$). On the occasions when no sign of solvent damage was visible the marker particles were usually found to be acceptably small, but insufficient in number to adequately delineate the fracture front. It seems, therefore, that there is a fundamental restriction on this technique for marking unless superior aerosols can be found.

4. Conclusions

The evaporation technique of fracture-front marking has proven to be successful and informative. The curved nature of the fracture front means that special care must be taken in the fracture mechanics analysis of the crack growth data. Ways of simplifying the information of crack front position produced by the methods described here are being explored with the aim of adopting existing fracture mechanics analysis based on the energy balance criterion to our current experiments.

Acknowledgements

This project is one of the activities supported by a Science Research Council Major Centre Grant, and one of the first to benefit from the provision of the scanning electron microscope/electron probe microanalysis machine for studies of polymer fracture and adhesive failures. One of us (JWT) acknowledges the University of Science of Malaysia for support through the ASTS Fellowship scheme.

References

1. P. MCINTYRE, *J. Soc. Env. Eng.* **13** (1974) 3.
2. E. H. ANDREWS and B. J. WALKER, *Proc. Roy. Soc.* **A235** (1971) 57.
3. J. W. TEH, J. R. WHITE and E. H. ANDREWS, *J. Mater. Sci.* **10** (1975) 1626.
4. B. J. WALKER, Ph. D. thesis, University of London (1969).
5. J. A. MANSON and R. W. HERTZBERG, *CRC Crit. Rev. Macromol. Sci.* **1** (1973) 433.

Received 18 July and accepted 15 September 1975.